Quantification of plant cardenolides by HPLC, measurement of Na^+/K^+-ATPase inhibition activity, and characterization of target enzymes

Georg Petschenka[a], Tobias Züst[b], Amy P. Hastings[c], Anurag A. Agrawal[c], and Georg Jander[d,*]

[a]Institute of Phytomedicine, University of Hohenheim, Stuttgart, Germany
[b]Department of Systematic and Evolutionary Botany, University of Zürich, Zürich, Switzerland
[c]Department of Ecology and Evolutionary Biology, Cornell University, Ithaca, NY, United States
[d]Boyce Thompson Institute, Ithaca, NY, United States
*Corresponding author: e-mail address: gj32@cornell.edu

Contents

1. Introduction 2
2. Rationale 6
3. Plant sample preparation 10
   3.1 Equipment 10
   3.2 Reagents 10
   3.3 Procedure 10
   3.4 Notes 11
4. HPLC analysis of cardenolide abundance 11
   4.1 Equipment 11
   4.2 Reagents 11
   4.3 Procedure 12
   4.4 Notes 12
5. Assays of Na^+/K^+-ATPase inhibition by plant extracts 14
   5.1 Equipment 14
   5.2 Reagents 14
   5.3 Procedure 15
   5.4 Notes 19
6. Inhibition of Na^+/K^+-ATPase from insect nervous tissue 20
   6.1 Equipment 20
   6.2 Reagents 20

Methods in Enzymology
ISSN 0076-6879
https://doi.org/10.1016/bs.mie.2022.08.003

6.3 Procedure 21
6.4 Notes 24
Acknowledgments 25
References 26

Abstract

The biosynthesis of cardiac glycosides, broadly classified as cardenolides and bufadienolides, has evolved repeatedly among flowering plants. Individual species can produce dozens or even hundreds of structurally distinct cardiac glycosides. Although all cardiac glycosides exhibit biological activity by inhibiting the function of the essential Na^+/K^+-ATPase in animal cells, they differ in their level of inhibitory activity. For within- and between-species comparisons of cardiac glycosides to address ecological and evolutionary questions, it is necessary to not only quantify their relative abundance, but also their effectiveness in inhibiting the activity of different animal Na^+/K^+-ATPases. Here we describe protocols for characterizing the amount and toxicity of cardenolides from plant samples and the degree of insect Na^+/K^+-ATPase tolerance to inhibition: (1) an HPLC-based assay to quantify the abundance of individual cardenolides in plant extracts, (2) an assay to quantify inhibition of Na^+/K^+-ATPase activity by plant extracts, and (3) extraction of insect Na^+/K^+-ATPases for inhibition assays.

1. Introduction

Cardiac glycosides are a structurally diverse group of natural products that inhibit the activity of Na^+/K^+-ATPase, an essential membrane ion transporter in almost all animal cells (Fig. 1). All cardiac glycosides have a

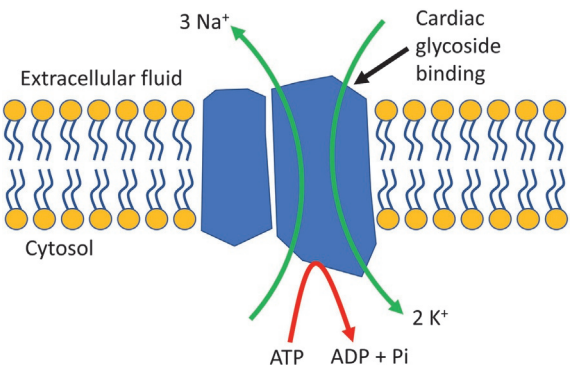

Fig. 1 Sodium-potassium pump is inhibited by cardiac glycosides. Na^+/K^+-ATPase is a membrane-bound protein complex found in animal cells. For every ATP that is consumed, three sodium ions are exported, and two potassium ions are imported. Inorganic phosphate that is released by the reaction can be measure spectrophotometrically. Binding of cardiac glycosides (cardenolides and bufadienolides) to Na^+/K^+-ATPase inhibits the enzyme function and the release of inorganic phosphate.

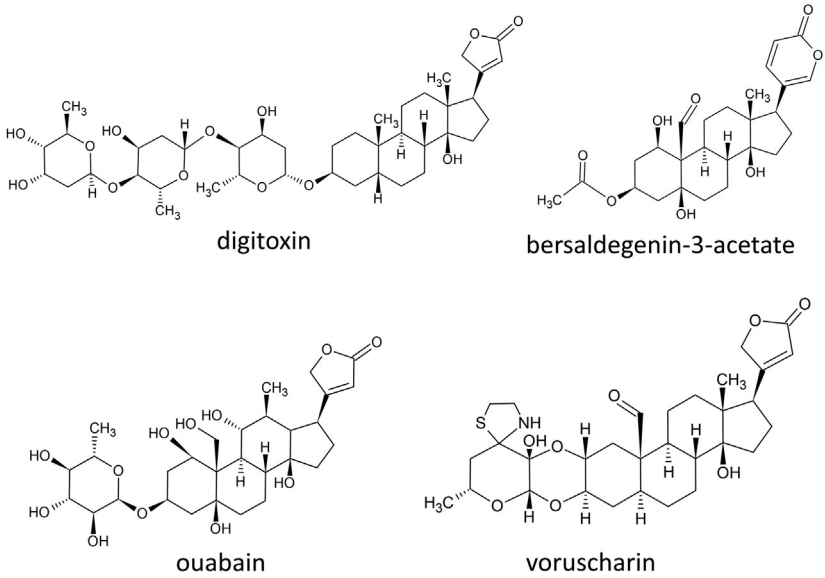

Fig. 2 Examples of cardiac glycosides. Digitoxin, a cardenolide found in *Digitalis purpurea*; ouabain, a cardenolide found in *Acokanthera schimperi*; voruscharin, a nitrogen- and sulfur-containing cardenolide found in *Asclepias curassavica*; and bersaldegenin-3-acetate, a bufadienolide found in *Kalanchoe daigremontiana*. The key difference between cardenolides and bufadienolides is the presence of a five- or six-membered lactone ring, respectively.

steroid core (5β,14β-androstane-3β14-diol; Fig. 2), which is essential for the binding of these compounds to animal Na^+/K^+-ATPase (Dzimiri, Fricke, & Klaus, 1987). Two classes of cardiac glycosides, cardenolides and bufadienolides (Fig. 2), have five- and six-membered lactone rings, respectively. Addition of sugar moieties, other modifications of the steroid core, as well as formation of stereoisomers, produce more than 500 known cardiac glycoside structures (Kreis & Müller-Uri, 2010; Melero, Medarde, & San Feliciano, 2000; Singh & Rastogi, 1970). Although most of these compounds have been identified from plants, they are also produced by toads (hence the bufadienolide name) and some beetles (Daloze & Pasteels, 1979; Qi, Zulfiker, Li, Good, & Wei, 2018; Steyn & van Heerden, 1998; Yoshida et al., 2020).

Given the toxicity of cardiac glycosides for most animals, it is likely that the primary function of these compounds in plants is protection against herbivory. Species in at least 16 plant families (Apocynaceae, Asparagaceae, Brassicaceae, Celastraceae, Crassulaceae, Euphorbiaceae, Fabaceae, Iridaceae, Malvaceae, Melianthaceae, Moraceae, Plantaginaceae, Ranunculaceae,

Santalaceae, Sterculaceae, and Zingiberaceae) independently evolved biosynthesis of cardiac glycosides, either in the form of cardenolides or bufadienolides (Afolabi, Adegoke, & Mathooko, 2011; Agrawal, Petschenka, Bingham, Weber, & Rasmann, 2012; Malcolm, 1991; Melero et al., 2000; Steyn & van Heerden, 1998). This convergent evolution of plant toxins that all target the same Na^+/K^+-ATPase in animal cells suggests strong selection for protection against herbivory, as well as the presence of common precursors in plant primary metabolism that facilitate the repeated evolution of similar compounds. Cardenolides occur in all plant parts, including floral nectar, although the composition of compounds typically differs between plant organs (Alani, Younkin, Mirzaei, Kumar, & Jander, 2021; Lopez-Goldar, Hastings, Zust, & Agrawal, 2022).

Plant species in which the biosynthesis and function of cardenolides have been studied extensively include foxgloves (*Digitalis* spp.; Plantaginaceae), milkweeds (*Asclepias* spp.; Apocynaceae) (Fig. 3A), and wallflowers (*Erysimum* spp.; Brassicaceae) (Fig. 3B). In the Apocynaceae, cardenolides are broadly distributed and likely represent an ancestral trait in this plant family (Agrawal, 2017; Agrawal, Salminen, & Fishbein, 2009). By contrast, *Erysimum* is one of only a small number of genera in the Brassicaceae that produce cardenolides, and likely represents a more recent evolution of this plant defensive trait (Moon, Rahman, Manir, & Ahamed, 2010; Züst et al., 2020). Cardenolide synthesis is likely a derived trait in other plant families as well, as typically only a small subset of the species in each plant family accumulate these compounds.

Several cardenolide-producing species, including foxglove (*Digitalis* spp.) (Kreis, 2017; Luckner & Wichtl, 2000) and wallflowers (Bock, 1577; Cordus, 1542; Dioscorides, 70AD; Jaretzky & Wilcke, 1932;

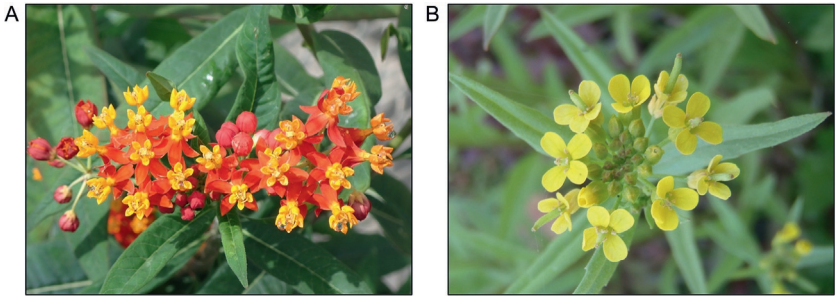

Fig. 3 Examples of cardenolide-producing plants. (A) *Asclepias curassavica* (tropical milkweed), Apocynaceae. (B) *Erysimum cheiranthoides* (wormseed wallflower), Brassicaceae.

Makarevich, Zhernoklev, Slyusarskaya, & Yarmolenko, 1994; Pliny the Elder, 77AD; Tabermontanus, 1588; Zhu, 1989), have been used extensively as traditional herbal medicines. The application of cardenolide-containing *Digitalis* extracts in the treatment of congestive heart failure, where partial inhibition of Na^+/K^+-ATPase activity causes a slower and stronger heartbeat, was first described in 1785 (Withering, 1785). The pharmaceutical digoxin, also known as Lanoxin, is listed on the World Health Organization's Model List of Essential Medications and is commercially derived from foxglove. More recent research shows that the therapeutic potential of cardenolides extends beyond the treatment of heart disease to include cancer, cystic fibrosis, ischemic stroke, neurodegenerative diseases, and viral infections (Ayogu & Odoh, 2020; Bejcek, Jurasek, Spiwok, & Rimpelova, 2021; Boff et al., 2019; Manna, Sreenivasan, & Sarkar, 2006; Mekhail et al., 2006; Mijatovic et al., 2006; Newman et al., 2020; Newman, Yang, Pawlus, & Block, 2008; Piccioni, Roman, Fischbeck, & Taylor, 2004; Pierre et al., 2007; Prassas & Diamandis, 2008; Reddy, Kumavath, Barh, Azevedo, & Ghosh, 2020; Shandell, Capatina, Lawrence, Brackenbury, & Lagos, 2022; Wang et al., 2006; Wong, Lingwood, Ostrowski, Cabral, & Cochrane, 2018). Thus, there is renewed interest in documenting the functional diversity of cardenolides and their possible medical applications.

Individual plant species can produce dozens to hundreds of structurally unique cardenolides. Wide variation in cardenolide solubility, stability, and binding site specificity may be necessary to protect plants against herbivores with different physiological characteristics. For instance, unique nitrogen-containing cardenolides in some milkweeds (*e.g.,* voruscharin; Fig. 2) provide protection against monarch butterfly caterpillars and seed bugs, which are otherwise highly resistant to these compounds (Agrawal et al., 2021; Agrawal et al., 2022). Both *in vivo* toxicity and *in vitro* Na^+/K^+-ATPase inhibition assays show that not all cardiac glycosides function in the same manner, and the most abundant compounds are not necessarily the most efficacious against a particular herbivore (Petschenka et al., 2018; Tverskoi et al., 2021).

Given the structural diversity and the variation in Na^+/K^+-ATPase inhibitory activity that is observed among different cardenolides, there is a need to implement uniform assays to: (1) estimate the abundance of individual cardenolide compounds in plant samples, and (2) compare the inhibition of diverse Na^+/K^+-ATPases by samples prepared from different plant species or tissue types.

2. Rationale

Cardenolides (Fig. 2) contain a single five-membered lactone ring, which has an absorbance maximum at 218 nm. No additional components of the cardenolides typically found in plants absorb at this wavelength. Therefore, equimolar amounts of different cardenolides will have approximately equivalent UV absorption. By preparing an HPLC standard curve with a commercially available cardenolide, *e.g.*, digitoxin (Fig. 2), it is possible to calculate the abundance of unknown cardenolides in plant samples that are separated using the same HPLC conditions. An assay for quantification of cardenolides in plant extracts (Züst, Petschenka, Hastings, & Agrawal, 2019) is described in Section 4.

Na^+/K^+-ATPase activity results in the hydrolysis of ATP and release of inorganic phosphate (Fig. 1), which can be detected spectrophotometrically, with an absorbance plateau between 700 and 900 nm (Fig. 4). When cardenolides are added to the reaction mix, Na^+/K^+-ATPase activity is inhibited and there is reduced accumulation of inorganic phosphate. Inhibition of Na^+/K^+-ATPase by cardenolides follows a sigmoid

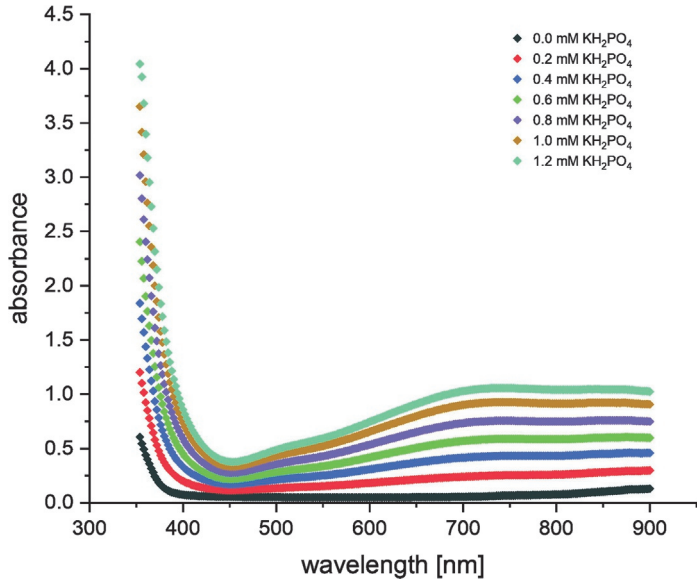

Fig. 4 Absorption spectrum of the blue color complex obtained by reduction of phosphomolybdic acid with ferrous sulfate. We recommend determination at 700 nm to achieve optimal resolution.

dose-response curve. By comparing the amount of cardenolides required to cause 50% Na^+/K^+-ATPase inhibition (IC_{50}), the assay can be used to: 1) quantify the cardenolide content of biological samples against a standard enzyme, 2) quantify the activity of different Na^+/K^+-ATPase enzymes against a standard cardenolide, *e.g.*, ouabain (Fig. 2), or 3) a combination of both (Figs. 5 and 6). An assay for inhibition of porcine Na^+/K^+-ATPase activity by plant extracts is described in Section 5. An assay to determine the inhibition of insect nervous tissue Na^+/K^+-ATPases by cardenolides is

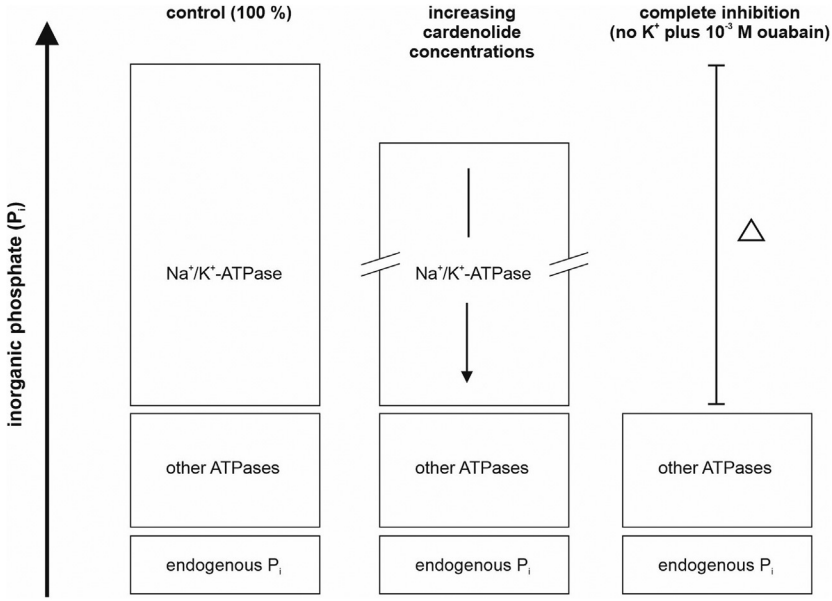

Fig. 5 Principle of Na^+/K^+-ATPase activity determination in crude enzyme preparations. Reactions contain several potential sources of inorganic phosphate (P_i) including P_i as a contaminant of samples, P_i from non-enzymatic hydrolysis of ATP (endogenous P_i), and P_i enzymatically released from ATP by Na^+/K^+-ATPase and other ATPases. Left column: under conditions of optimal ionic composition (Na^+, K^+, Mg^{2+}), pH, and ATP, Na^+/K^+-ATPase is fully active. Central column: Na^+/K^+-ATPase is specifically inhibited by various concentrations of cardiac glycosides leading to reduced P_i. Right column: Na^+/K^+-ATPase is fully inhibited due to a high concentration of the cardiac glycoside ouabain and a lack of K^+. The difference in absorbance between left and right (Δ) represents Na^+/K^+-ATPase activity. Combining a buffer regime free of K^+ with a high concentration of ouabain (*e.g.*, 10^{-3} M) eliminates residual Na^+/K^+-ATPase activity due to potentially contaminating K^+ from the sample or enzyme preparation. In addition, cardiac glycoside tolerant forms of Na^+/K^+-ATPase having residual activity at high concentrations of cardenolides under optimal conditions will be fully inhibited due to the lack of K^+, combined with the high concentration of inhibitor.

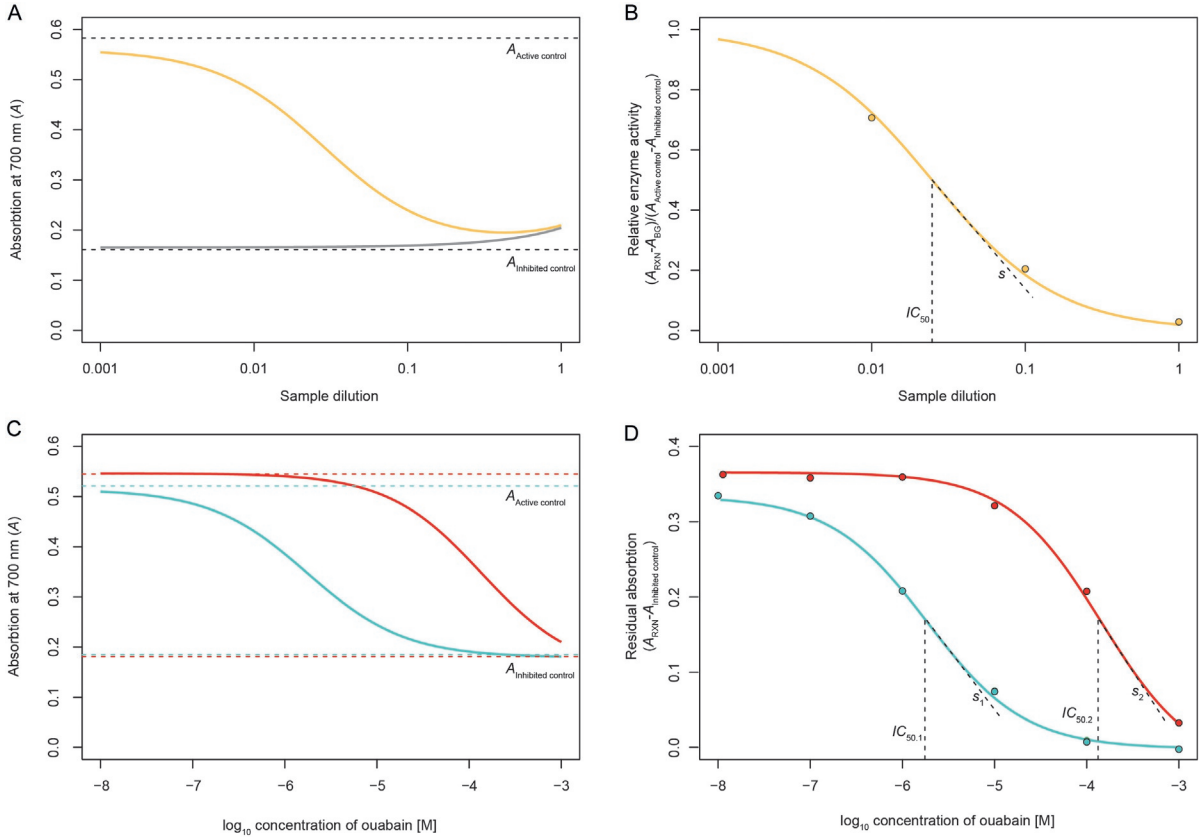

Fig. 6 See figure legend on opposite page.

described in Section 6. Quantification of cardenolides by Na^+/K^+-ATPase inhibition was originally described by Klauck and Luckner (1995) and has subsequently been modified (Petschenka & Agrawal, 2015; Züst et al., 2019). The *in vitro* assay of Na^+/K^+-ATPase described here (for the original description, see Petschenka et al., 2013) is based on work from several prior authors, including: Moore and Scudder (1986), Mori et al. (2009), and Taussky and Shorr (1953).

The sigmoid dose-response curve of Na^+/K^+-ATPase inhibition by cardenolides (Fig. 6) can be estimated using a logistic model, where the absorption A at concentration x is a function of the absorption by an uninhibited (K) and fully inhibited enzyme (L), the concentration at the inflection point, IC_{50} (equal to the concentration/dilution required to inhibit enzyme activity by 50%), and a scaling coefficient s:

$$A_x = \frac{K - L}{\left(1 + e^{\left(\frac{IC_{50} - x}{s}\right)}\right)} - L$$

Other equivalent approaches and proprietary software solutions exist to estimate a sigmoid dose-response curve, but the above function can easily be fitted using the open-source statistical software R. If all parameters are to

Fig. 6 Sigmoid dose-response curves. (A) Phosphate absorption signal of porcine Na^+/K^+-ATPase reactions inhibited by a leaf extract with unknown cardenolide content at different dilutions (orange), and the unspecific background absorption of the same reaction mixture and leaf extract inhibited by a high dose of ouabain and a lack of KCl (gray). Strongly colored extracts may cause even stronger background absorption. Absorption of the fully active and fully inhibited enzyme can be approximated from control reactions (dashed lines). Note that leaf extracts may change enzyme activity compared to control reactions, thus estimating of the asymptotes directly from the inhibition series can improve model fit. (B) Relative enzyme activity estimated by subtracting background absorption from each reaction and dividing by the absorption of a fully active enzyme reaction. The upper and lower asymptote of the sigmoid function are fixed at 1 and 0, respectively, allowing to estimate the extract dilution required to achieve 50% inhibition (x_{mid}) and the function shape (s) from as few as three dilutions. (C) Phosphate absorption signal of Na^+/K^+-ATPase reactions inhibited by a concentration series of the cardenolide ouabain, using brain extracts from a susceptible (*Euploea core*, blue) and a cardenolide-resistant (*Danaus plexippus*, red) insect. Absorption of the fully active and fully inhibited enzyme can be approximated from control reactions in separate wells (dashed lines). (D) Relative enzyme activity estimated by dividing the absorption of each reaction by the absorption of its respective control. The upper and lower asymptote of the sigmoid function are fixed at 1 and 0, respectively. Sampling of more ouabain concentrations allows for a more accurate estimation of curve shapes.

be estimated, a minimum of five different concentrations per biological sample need to be assayed. To reduce the number of reactions, uninhibited and fully inhibited activity can be estimated from additional reactions (one value per microtiter plate) to calculate relative activity of each sample well before curve fitting (Figs. 5 and 6) by allowing K and L to be fixed to 1 and 0, respectively. This simplified approach is implemented in Section 5 to allow the processing of more biological samples in each individual microtiter plate. However, the assaying of more concentrations is recommended, particularly if different insect enzymes are being compared.

3. Plant sample preparation

3.1 Equipment

- Lyophilizer (Labconco, Kansas City, MO, USA)
- Savant Speedvac rotary vacuum concentrator (ThermoFisher, Waltham, MA, USA)
- FastPrep-24 homogenizer (MP Biomedicals, Irvine, CA, USA)
- Microcentrifuge (Eppendorf, Hamburg, Germany)

3.2 Reagents

- Liquid nitrogen
- Methanol
- FastPrep beads (2.3 mm zirconia/silica beads, MP Biomedicals, Irvine, CA, USA)
- 2 mL screw-cap vials (Sarstedt, Nürmbrecht, Germany)
- Digitoxin (Sigma Aldrich, St. Louis, MO, USA)

3.3 Procedure

1. Harvest 0.5 to 1 g plant material.
2. Freeze plant material in liquid nitrogen (See Note 1).
3. Dry plant material overnight in a lyophilizer.
4. Weigh out ~50 mg dry plant material into a 2 mL screw cap vial.
5. Add 1.25 mL 100% methanol and ~30 FastPrep beads to each sample.
6. Agitate samples twice for 45 s at a speed of 6.5 m/s on a FastPrep-24 homogenizer.
7. Centrifuge samples for 12 min at 15,000 × g in a microcentrifuge.
8. Collect supernatants.
9. Extract pellet again with 1.25 mL 100% methanol. (See Note 2).

10. Centrifuge samples for 12 min at 15,000 × *g* in a microcentrifuge.
11. Collect supernatant and combine with supernatant from Step 8, mix well.
12. Split supernatant into two aliquots, 2 mL to be used for HPLC analysis (Section 4) and 0.25 mL to be used in the Na^+/K^+-ATPase assays (Section 5) (see Note 3).
13. Add 20 μg of the digitoxin cardenolide to the samples that will be used for HPLC analysis.
14. Evaporate all samples to dryness in a rotary vacuum concentrator.

3.4 Notes

1. Samples frozen within a few hours of collection still allow detection of cardenolides.
2. The second extraction (Steps 9–11) may not be necessary for all sample types.
3. If only HPLC analysis or only Na^+/K^+-ATPase assays are planned, it is not necessary to prepare both sample types.

4. HPLC analysis of cardenolide abundance

4.1 Equipment

- Agilent 1100 HPLC (Agilent, Santa Clara, CA, USA)
- Diode array detector (Agilent, Santa Clara, CA, USA)
- Microcentrifuge (Eppendorf, Hamburg, Germany)

4.2 Reagents

- Gemini C18 reversed-phase column (3 μm, 150 × 4.6 mm) (Phenomenex, Torrance, CA, USA)
- Acetonitrile
- HPLC-grade water
- 0.2 μm syringe filter with Kinesis PTFE membrane (Cole Parmer, Vernon Hills, IL, USA)
- 2 mL screw cap HPLC vials (ThermoFisher, Waltham, MA, USA)
- Caps for HPLC vials (ThermoFisher, Waltham, MA, USA)
- 300 μL polyspring HPLC vial inserts (ThermoFisher, Waltham, MA, USA)

4.3 Procedure

1. Resuspend dried aliquots for HPLC from Section 3 in 300 μL methanol. (See Notes 1,2)
2. Filter samples using a 0.2 μm syringe filter with a PTFE membrane. (See Note 3)
3. Add samples to polyspring inserts in HPLC vials.
4. Inject 15 μL of each sample into the HPLC for separation on a C18 reversed phase column.
5. Run HPLC with a constant flow of 0.7 mL/min using the following gradient of acetonitrile and water: 0–2 min at 16% acetonitrile; 2–25 min from 16% to 70% acetonitrile; 25–30 min from 70% to 95% acetonitrile; 30–35 min at 95% acetonitrile; followed by 10 min reconditioning at 16% acetonitrile. (See Notes 4–6)
6. Record UV absorbance spectra of eluted compounds at 200 to 400 nm.
7. Calculate areas of peaks with an absorption maximum in the 214 to 222 nm range (Fig. 7). (See Note 7)
8. Calculate cardenolide concentrations by relating peak areas to a calibration curve created with the internal standard, digitoxin. (See Note 8)

4.4 Notes

1. Some samples with a high content of UV-absorbing compounds, such as *Apocynum* and *Digitalis* leaf extracts, benefit from a lead acetate precipitation step (Brower, Seiber, Nelson, Lynch, & Tuskes, 1982).
2. Seed and animal samples benefit from being defatted by liquid-liquid extraction with hexane.
3. In Step 2, it is important to avoid using nylon filter membranes, as digitoxin can adsorb to these membranes if it is not diluted in methanol (*e.g.*, in acetonitrile-water).
4. The chromatographic separation method described here is optimized for use on HPLC instruments and has broad applicability across plant species. The method run time can be substantially reduced using core-shell or UHPLC columns with smaller pore sizes, and by optimizing the gradient conditions for each species of interest.
5. For certain column conditions and polar cardenolides, in particular, there are benefits to injecting the samples in 16:16:68 methanol:acetonitrile:water, rather than 100% methanol (Agrawal et al., 2021).
6. Cardenolides can also be detected by HPLC-MS, which provides greater specificity for compound identification (Agrawal et al., 2021;

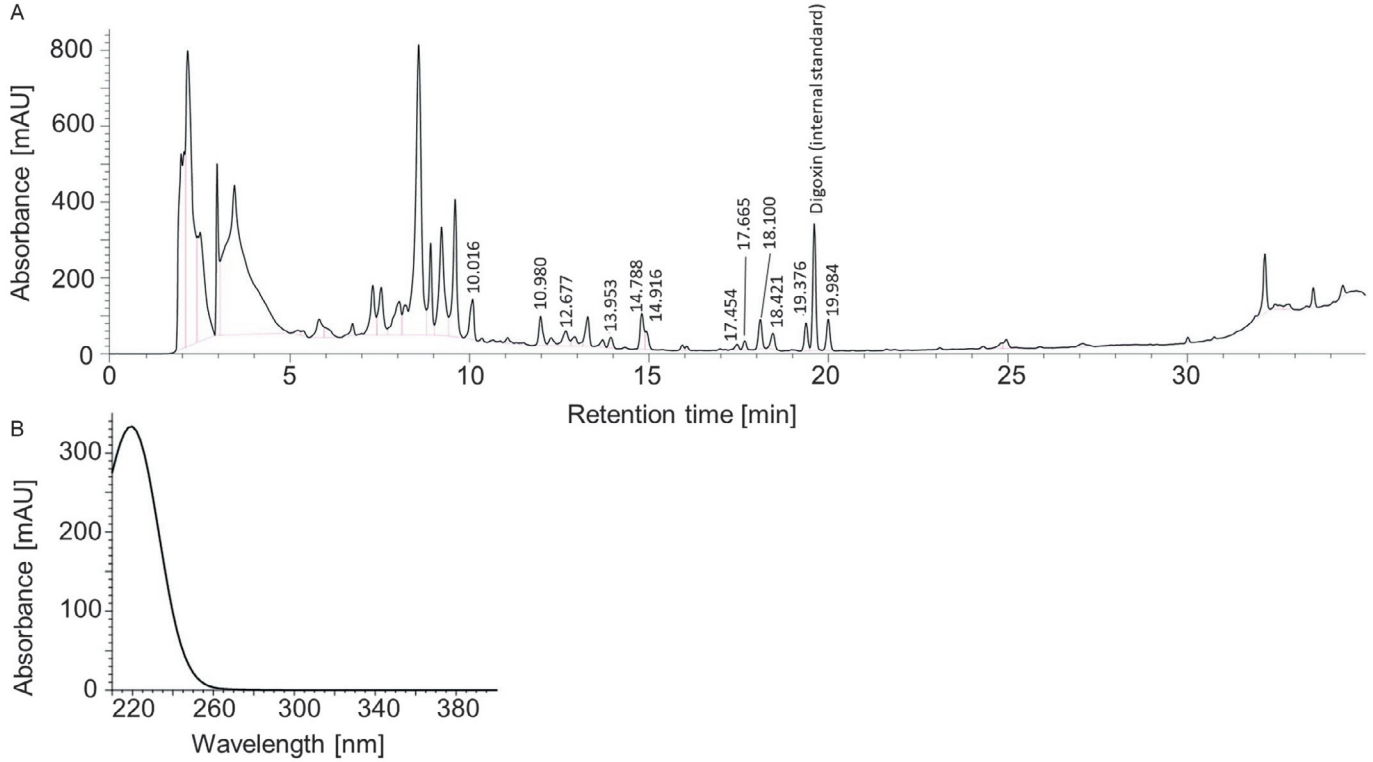

Fig. 7 (A) Representative HPLC-UV chromatogram of *Asclepias curassavica*. Peaks with the typical absorption profile of cardenolides (B) are marked with their retention times. HPLC-UV conditions are described in the text.

Züst et al., 2020). However, in the absence of standards for each cardenolide, absolute quantification is not possible from MS signals alone.

7. Peaks showing a single absorption maximum in the 214 to 222 nm UV range, corresponding to an unsaturated lactone ring, are considered representative of cardenolides in this assay. All cardenolides contain a single lactone ring and do not have additional components that absorb in the 214 to 222 nm range. Therefore, equimolar amounts of different cardenolides have approximately equivalent UV absorption. A sample chromatogram produced using the HPLC-UV conditions described in the protocol is shown in Fig. 7
8. Each injected sample contains the equivalent of ~2 mg dried plant material and 1 μg digitoxin. Therefore, the concentration of each cardenolide in the original plant sample can be calculated as: concentration (μg/mg dried plant material) = peak area (cardenolide of interest)/peak area (digitoxin)/2.

5. Assays of Na^+/K^+-ATPase inhibition by plant extracts

5.1 Equipment

- Spectramax 190 microplate spectrophotometer (Molecular Devices, San Jose, CA, USA)
- BioShake Iq microplate shaker (Quantifoil Instruments, Jena, Germany)
- Cole-Parmer sonicator (Antylia Scientific, Vernon Hills, IL, USA)
- Multichannel pipette (ThermoFisher, Waltham, MA, USA)

5.2 Reagents

- 96-well microtiter plates (Sarstedt, Nümbrecht, Germany)
- 1.5 mL microcentrifuge tubes (ThermoFisher, Waltham, MA, USA)
- Na^+/K^+-ATPase from pig (*Sus scrofa*) cerebral cortex (Sigma-Aldrich, MO, USA) Chemicals, all available from Sigma Aldrich, St. Louis, MO, USA:
- Ouabain (octahydrate)
- Dimethylsulfoxide (DMSO)
- Imidazol
- Sodium chloride (NaCl)
- Magnesium chloride hexahydrate ($MgCl_2 \cdot 6H_2O$)
- Potassium chloride (KCl)

- Adenosine 5′-triphosphate di(tris) salt hydrate (ATP)
- Sodium dodecyl sulfate (SDS)
- Antifoam A emulsion
- Deionized water
- 10 N H_2SO_4
- $(NH_4)_6Mo_7O_{24}{\cdot}4H_2O$
- Iron(II) sulfate heptahydrate
- Concentrated HCl
- Tris Base

5.3 Procedure

1. Add 40 μL 100% DMSO to each dried aliquot of plant material for the Na^+/K^+-ATPase assays (from Section 3).
2. Sonicate sample twice for 5 min.
3. Add 160 μL water to bring sample to 20% DMSO, briefly vortex, and sonicate once for 5 min. (See Note 1)
4. Centrifuge sample for 12 min at 15,000 × *g* in a microcentrifuge to precipitate particles.
5. Collect supernatant into fresh 1.5 mL microcentrifuge tube.
6. Each biological sample is assayed at a minimum of three concentrations. For each sample, use 20% DMSO to make serial 10-fold dilutions (*e.g.*, 1, 0.1, and 0.01) of the plant extracts in 1.5 mL microcentrifuge tubes. (See Note 2)
7. To control for coloration of leaf extracts, each concentration series is run in both the presence of KCl (Reaction Mastermix) and absence of KCl but with 0.2 mM ouabain (Inhibited Control Reaction Mastermix) (See Note 3). Add 20 μL of each concentration of a sample dilution series to two individual wells of a 96-well microtiter plate (*e.g.*, orange and green wells A1 to G12 in Fig. 8A, respectively).
8. Add 20 μL 20% DMSO to each of three wells of the plate designated as full-activity controls, (*e.g.,* wells H1 to H3 in Fig. 8A) and three wells designated as fully-inhibited controls (*e.g.,* wells H10 to H12 in Fig. 8A).
9. Prepare a standard curve by adding 20 μL ouabain at each of the following concentrations: 5×10^{-3}, 5×10^{-4}, 5×10^{-5}, 5×10^{-6}, 5×10^{-7}, 5×10^{-8} M, in 20% DMSO. These will be diluted 5× in the assay, so final ouabain concentrations will be 10^{-3} to 10^{-8} M. (*e.g.,* wells H4 to H9 in Fig. 8A).

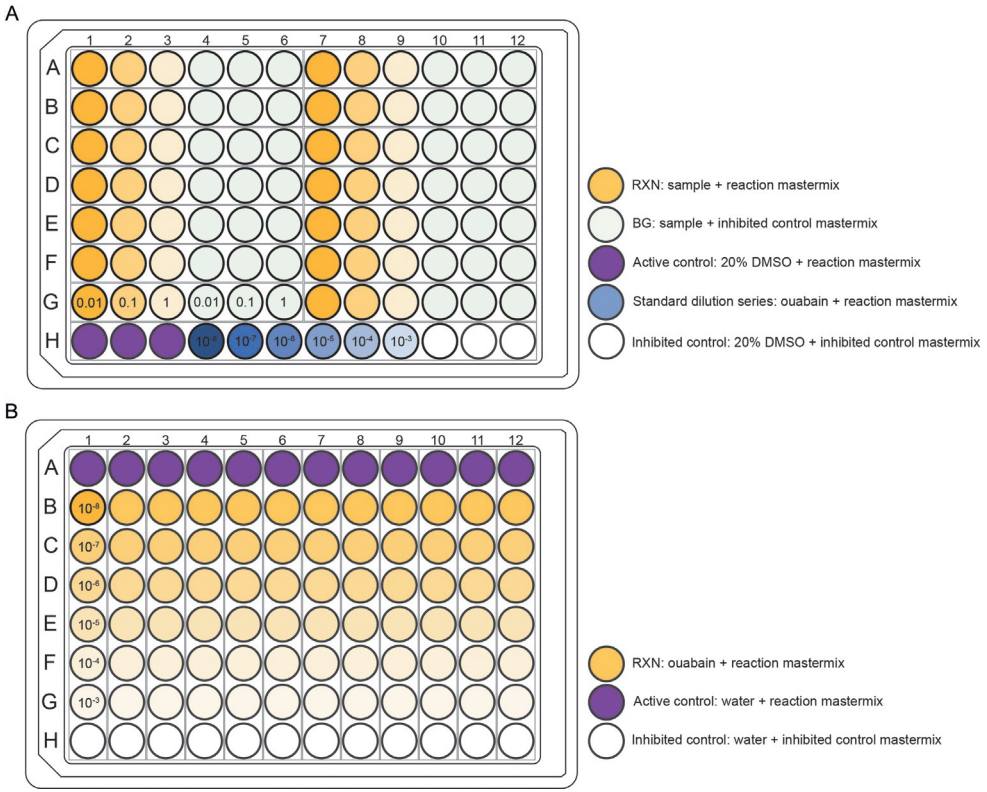

Fig. 8 Sample layout of a microtiter plate for Na^+/K^+-ATPase assays. (A) Sample layout for the assaying of 14 cardenolide-containing plant extracts using inhibition of porcine Na^+/K^+-ATPase. Each extract is run at three dilutions, once with active reaction mastermix to measure enzyme activity (orange), and once with an inhibited control mastermix lacking KCl but containing 0.2 mM ouabain to quantify background absorption in the absence of enzymatic activity due to extract coloration (green). Each plate additionally contains three active controls (purple), a standard series with six dilutions of the cardenolide ouabain (blue), and three inhibited controls (white). Due to plate-level differences in enzyme activity, splitting of wells belonging to one replicate across several plates is not recommended. Technical replicates of the same extract may be assayed if very high accuracy in determination of activity is required, but biological replicates may be more meaningful. (B) Sample layout for the assaying of 12 enzyme samples by a cardenolide (*e.g.*, ouabain) concentration series. Each enzyme sample is run at six cardenolide concentrations (orange), and for each sample a fully active control (purple) and a fully inhibited control (lacking KCl but containing 0.2 mM ouabain, white) is included.

10. Cover plate and set aside.
11. Prepare porcine ATPase by dissolving it in deionized water, to 0.05 units/mL (See Note 4).
12. On ice, make up an Na^+/K^+-ATPase Reaction Mastermix and an Inhibited Control Reaction Mastermix for your plate, by mixing either Reaction Buffer (Table 1A, 25 µL per sample) or Inhibited Control

Table 1 Stock solutions for Na+/K+-ATPase assays.

(A) Na^+/K^+-ATPase reaction buffer			(B) Inhibited control buffer		
Compound	**g/100 mL**	**Concentration**	**Compound**	**g/100 mL**	**Concentration**
NaCl	2.34 g	400 mM	NaCl	2.34 g	400 mM
MgCl2	0.269 g	16 mM	$MgCl_2 \cdot 6H_2O$	0.325 g	16 mM
Imidazole	1.36 g	200 mM	Imidazole	1.36 g	200 mM
KCl	0.596 g	80 mM	Ouabain-octahydrate	0.058 g	0.8 mM
Bring to 100 mL with deionized water, adjust pH to 7.4 with concentrated HCl, and store at room temperature.			Bring to 100 mL with deionized water, adjust pH to 7.4 with concentrated HCl, and store at room temperature.		

(C) ATP stock solution	(D) Taussky-Shorr stock solution
Adenosine 5′-triphosphate di(tris) salt hydrate	500 mL 10 N H_2SO_4
	50 g $(NH_4)_6Mo_7O_{24} \cdot 4H_2O$
Calculate the molecular weight based on the certificate of analysis (molecular weight depends on the amount of included water) and make a 10 mM solution in deionized water, adjust to pH 6.5 with 1 M Tris Base, and store aliquots at −20 °C.	Mix 400 mL 10 N H_2SO_4 with 50 g $(NH_4)_6Mo_7O_{24} \cdot 4H_2O$ in a 1 L beaker under constant stirring, transfer into a 500 mL volumetric flask when completely dissolved, wash 1 L beaker quantitatively with small amounts of 10 N H_2SO_4 to achieve 500 mL total volume in the flask. See Taussky and Shorr (1953).

(E) SDS stock solution
10 g Molecular biology grade SDS
50 µL Antifoam A emulsion
Dissolve ingredients in deionized water, bring volume to 100 mL, store at room temperature, invert before use (has tendency to sediment).

Buffer (Table 1B, 25 µL per sample), ATP stock solution (Table 1C, 25 µL per sample), and porcine ATPase (30 µL per sample), for a total volume of 80 µL per sample. Mix very well by vortexing followed by a short spin in a microcentrifuge, then keep on ice to prevent ATPase activity.

13. Using a multichannel pipette, add 80 µL of the appropriate Mastermix to each well (samples, standards, and controls). Place plate on microplate shaker and do 5–6 quick mixes at 1600 rpm to mix wells thoroughly.
14. Incubate plates at 37 °C for 20 min on the microplate shaker (cover plates to reduce evaporation), shaking slowly at 200 rpm
15. Make up Taussky-Shorr staining solution fresh by diluting 1 mL 10% ammonium molybdate stock solution (Table 1D) with 7 mL deionized water, vortex to mix, and then add 500 mg iron(II) sulfate heptahydrate, mix until dissolved, and bring volume up to 10 mL with deionized water.
16. Stop the enzymatic reactions by adding 100 µL SDS stock solution (Table 1E) to each well of the plate using a multichannel pipette and mix at least 3 times with the pipette
17. Add 100 µL Taussky-Shorr staining solution to each well using a multichannel pipette and mix at least 6 times with the pipette to ensure homogeneity. Incubate the plate at room temperature for 10 min.
18. Measure absorbance at 700 nm in a microplate spectrophotometer. (See Notes 5 and 6)
19. Correct absorbance values of each reaction well by subtracting its respective background well (lacking KCl and with ouabain, see Step 13).
20. Correct absorbance value of full-activity control samples by subtracting the absorbance of fully inhibited control samples, *e.g.*, in the layout in Fig. 8A, subtract the reading from A4 from that from A1.
21. Calculate the residual enzymatic activity by dividing each background-corrected absorbance of each sample reaction by the background-corrected absorbance of full-activity controls (*e.g.*, in Fig. 8A, subtract H10-H12 from H1-H3 and then calculate the mean) to calculate the percentage relative to Na^+/K^+-ATPase activity in non-inhibited controls. Instead, if four or more concentrations per sample are assayed, full and residual enzymatic activity (*K* and *L*) can be estimated directly from background-corrected sample absorbances.

22. Estimate the sigmoid dose-response curve (Fig. 6) for each sample by fitting a 2-parameter logistic model using generalized least squares (*gnls* function in the *nlme* library for R). (See Note 7)
23. Extract the relative dilution at the inflection point (IC_{50}, residual enzymatic activity of 50%).
24. Use the ouabain dilution series to calculate the ouabain equivalents in the undiluted sample, *i.e.*, the amount of ouabain that is required to achieve equivalent inhibition of the porcine Na^+/K^+-ATPase. (See Note 8)

5.4 Notes

1. Most cardenolides are also soluble in 10% DMSO, but we have chosen to use 20% DMSO in assays in order to avoid solubility issues for some very non-polar compounds. DMSO can inhibit enzymatic activity, but this unspecific effect is still mostly negligible at 20% concentration. If using different DMSO concentrations, be sure to do the same for plant extracts, standards, and controls. Excessively high DMSO concentrations can inhibit enzymatic activity.
2. Three dilutions of the samples are a minimum for estimating IC_{50}. The sample layout in Fig. 8A allows for the assaying of 14 biological samples. Five to six dilutions will give a more accurate result at the cost of fewer samples per microplate.
3. Based on past experience, the porcine Na^+/K^+-ATPase is completely inhibited at 0.1 mM ouabain, so a final concentration of 0.2 mM should be enough for the fully inhibited control in this experiment.
4. Frozen aliquots of porcine Na^+/K^+-ATPase at a concentration of 1 unit/mL in individual 1.5 mL tubes can be stored at −80 °C. Dilution of stock solution prior to storage at −80 °C may result in loss of activity.
5. The absorbance profile has a plateau at 700–900 nm, but 700 nm is optimal (the baseline is increasing at >800 nm).
6. P_i emission and absorbance values show a linear relationship from 0 to 1.2 mM P_i in the reaction. To ensure that measured absorbance values fall within the linear range of Pi detection, a calibration curve based on KH_2PO_4 in deionized water (0.2 mM intervals, 100 µL per well for each concentration) can be used as a standard on the same plate. KH_2PO_4 standards are processed in the same way as other samples.

7. Use of the *gnls()* function treats each sample dilution series as independent, giving individual noisy datapoints more weight to distort the curve fitting. Instead, curves can be fitted within a mixed-effects model framework, in which each sample dilution series is estimated as a random deviate from a universal mean curve. This approach can be implemented using the *nlme()* function in the nlme package for R. Based on prior experience, *nlme* fits are more robust with respect to technical noise, but may be more challenging to fit. Sample R code is provided in the supplementary materials. Other software, *e.g.*, Origin Pro, GraphPad Prism, or the Solver Add-in for Microsoft Excel can also be used for curve fitting.
8. In addition to ouabain, other commercially available cardenolides can be used as standards for comparison of the enzymatic activity. Due to the superior water-solubility of ouabain compared to most other commercially available cardenolides, it does not require the use of organic solvents such as DMSO.

6. Inhibition of Na^+/K^+-ATPase from insect nervous tissue

6.1 Equipment

- Lyophilizer (Labconco, Kansas City, MO, USA)
- 1 mL all-glass tapered tissue grinder (Wheaton, Millville, NJ, USA)
- Spectramax 190 microplate spectrophotometer (Molecular Devices, San Jose, CA, USA)
- BioShake Iq microplate shaker (Quantifoil Instruments, Jena, Germany)
- Cole-Palmer sonicator (Antylia Scientific, Vernon Hills, IL, USA)
- Multichannel pipette (ThermoFisher, Waltham, MA, USA)
- Dumont no. 5 tweezers (Manufactures D'Outils Dumont SA, Montignez, Switzerland)

6.2 Reagents

- Fresh or live-frozen insects
- 96-well microtiter plates (Sarstedt, Nümbrecht, Germany)
- 1.5 mL microcentrifuge tubes (ThermoFisher, Waltham, MA, USA)
- Deionized water
- Parafilm
- Chemicals, all available from Sigma Aldrich, St. Louis, MO, USA:

- Ouabain (octahydrate)
- Imidazol
- Sodium chloride (NaCl)
- Magnesium chloride hexahydrate ($MgCl_2 \cdot 6H_2O$)
- Potassium chloride (KCl)
- Adenosine 5′-triphosphate di(tris) salt hydrate
- Sodium dodecyl sulfate (SDS)
- Antifoam A emulsion
- 10 N H_2SO_4
- $(NH_4)_6Mo_7O_{24} \cdot 4H_2O$
- Iron(II) sulfate heptahydrate
- Concentrated HCl
- Tris Base

6.3 Procedure

1. Dissect brain and thoracic ganglia (when possible) under ice-cold deionized water in a black microscopy bowl pre-chilled on ice using Dumont no. 5 tweezers (Fig. 9). (See Notes 1–3)
2. Rinse dissected material in deionized water.
3. If necessary, pool dissected tissues from several insects to obtain sufficient nervous system material. The number of specimens needed may vary substantially, even between closely related species. (See Note 4)
4. Grind insect tissue in deionized water in a glass grinder by several rounds of grinding. Chill grinder on ice in between.
5. Freeze samples at −80 °C in open 1.5 mL microcentrifuge tubes covered with stretched Parafilm and punctured with a needle for gas exchange.
6. Lyophilize samples overnight.
7. Store lyophilized samples at −80 °C until they are used for assays.
8. If ouabain is being used as the inhibitor (See Note 5), prepare fully active and fully-inhibited controls in rows A and H, respectively, by adding 20 μL of water (Table 1B, but see Note 6) to each well (Fig. 8B). (See Note 7)
9. In rows B to G, add 20 μL of a ouabain concentration series at each of the following concentrations: 5×10^{-3} M, 5×10^{-4} M, 5×10^{-5} M, 5×10^{-6} M, 5×10^{-7} M, 5×10^{-8} M, in water (Fig. 8B).
10. Cover plate and set aside.

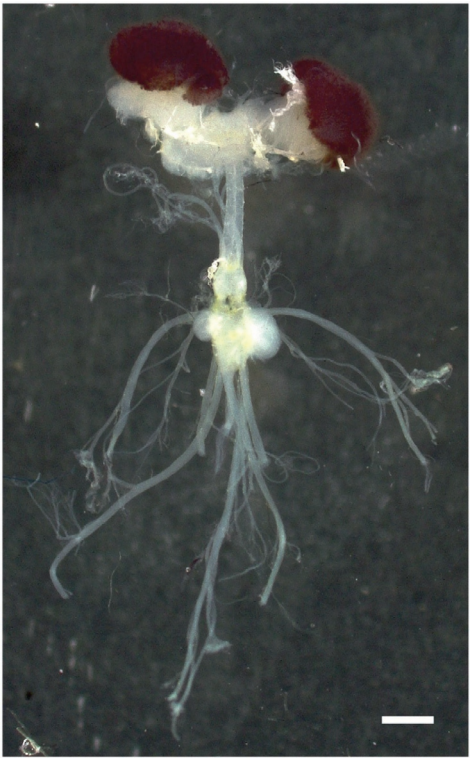

Fig. 9 Insect brain dissection. Brain and thoracic ganglia dissected from a monarch butterfly (*Danaus plexippus*), stored at −80 °C. The dissection was carried out in deionized water and tissue is starting to disintegrate, likely due to osmosis.

11. Add water to the lyophilized insect nervous system tissue, with the volume depending on how many assays need to be run. (See Note 8)
12. Sonicate samples twice for 5 min, being sure that samples remain cold.
13. Centrifuge samples for 3 min at $5000 \times g$ in a microcentrifuge to precipitate particles.
14. Collect water-soluble supernatant containing insect Na^+/K^+-ATPase into fresh tubes.
15. On ice, make up an Na^+/K^+-ATPase Reaction Mastermix and an Inhibited Control Reaction Mastermix for each enzyme sample, by mixing either Reaction Buffer (Table 1A, 25 µL per sample) or Inhibited Control Buffer (Table 1B, 25 µL per sample), ATP stock solution (Table 1C, 25 µL per sample), and insect ATPase preparation

(30 μL per sample), for a total volume of 80 μL per sample. Mix very well by vortexing followed by a short spin in a microcentrifuge, then keep on ice to prevent ATPase activity.

16. Add 80 μL of the appropriate Mastermix to each well (enzyme samples and controls). Place plate on microplate shaker and do 5–6 quick mixes at 1600 rpm to mix wells thoroughly.
17. Incubate plates at 37 °C for 20 min on the microplate shaker (cover plates to reduce evaporation), shaking slowly at 200 rpm.
18. Make up Taussky-Shorr staining solution fresh by diluting 1 mL 10% ammonium molybdate stock solution (Table 1D) with 7 mL deionized water, vortex to mix, and then add 500 mg iron(II) sulfate heptahydrate, mix until dissolved, and bring volume up to 10 mL with deionized water.
19. Stop the enzymatic reactions by adding 100 μL SDS stock solution (Table 1E) to each well of the plate using a multichannel pipette and mix at least 3 times with the pipette.
20. Add 100 μL Taussky-Shorr staining solution to each well using a multichannel pipette and mix at least 6 times with the pipette to ensure homogeneity. Incubate the plate at room temperature for 10 min.
21. Measure absorbance at 700 nm in a microplate spectrophotometer. (See Notes 9, 10)
22. Correct for background absorbance values of all samples by subtracting the absorbance of fully inhibited control samples, *e.g.*, Row H (lacking KCl and with ouabain, see Step 15) in the layout in Fig. 8B, from the corresponding samples in Rows A to G.
23. Calculate the residual enzymatic activity by dividing each background-corrected absorbance of each sample reaction by the background-corrected absorbance of full-activity controls (*e.g.*, Row A in Fig. 8B) to calculate the percentage relative to Na^+/K^+-ATPase activity in non-inhibited controls. Alternatively, given that there are six concentrations of ouabain in this assay (Rows B to G), full and residual enzymatic activity (*K* and *L*) can be estimated directly from background-corrected sample absorbances.
24. Estimate the sigmoid dose-response curve (Fig. 6) for each sample by fitting a 2-parameter logistic model using generalized least squares (*gnls* function in the *nlme* library for R). (See Note 11)
25. Extract the relative dilution at the inflection point to calculate the IC_{50} (residual enzymatic activity of 50%). (See Note 12)

6.4 Notes

1. Live insects can be killed by freezing and can be stored frozen at −80 °C prior to dissection of nervous system tissue. Use of tight plastic envelopes or tubes will prevent samples from drying out. Na^+/K^+-ATPase is likely to remain stable for several months or years at −80 °C.
2. The brain and thoracic ganglia are a major site of Na^+/K^+-ATPase expression in many insects, and are thus a good source of material for enzymatic assays (Petschenka, Offe, & Dobler, 2012). Active Na^+/K^+-ATPase preparations have been obtained from nervous tissue of Orthoptera (Acrididae, Pyrgomorphidae), Coleoptera (Cerambycidae, Chrysomelidae), Diptera (Agromyzidae, Drosophilidae), Heteroptera (Lygaeidae), and Lepidoptera (Erebidae, Nymphalidae, Sphingidae).
3. In addition to nervous tissue, active preparations can also be obtained from the rectum of some insects such as orthopterans. For small insects, such as leaf miner flies or *Drosophila*, entire heads can be used.
4. The amount of required tissue material needs to be assessed for each system. Differences of absorbance between non-inhibited Na^+/K^+-ATPase and background (no-KCl, with ouabain) phosphate should be >0.2 to obtain reliable low-noise data. For dissected *Danaus plexippus* brains, 0.75 brain/1.5–2 mL water will be sufficient for 45–60 reactions (*i.e.*, 60–80 reactions per brain). Whole heads of *Drosophila melanogaster* at a ratio of 12.5 heads/450 μL will be sufficient for ~14 reactions (*i.e.*, one reaction per head). *Oncopeltus fasciatus* brains and thoracic ganglia at ~6–10 brains/600 μL will allow for ~18 reactions (*i.e.*, 2–3 reactions per brain). *Tetraopes* brains at ~10 brains/500 μL will allow for ~15 reactions (*i.e.*, 1.5 reactions per brain).
5. For less water-soluble cardiac glycosides, up to 20% DMSO can be used. However high concentrations of DMSO will inhibit enzyme activity and may also interfere with binding of cardiac glycosides to the active site.
6. Although the MasterMix (Table 1B) contains 0.8 mM ouabain (for a final concentration of 0.2 mM, which is fully inhibitory for porcine Na^+/K^+-ATPase), for insect enzyme assays, we recommend using the highest ouabain concentration possible. Based on the water solubility of ouabain, this would be 10^{-2} M in the stock solution. If this buffer is diluted 4×, the final concentration in the assay will be $2.5 * 10^{-3}$ M. This is particularly important when generating

fully-inhibited controls for Na^+/K^+-ATPase assays involving tissue from insects such as monarchs and milkweed bugs, which have elevated, and often unknown levels of cardenolide resistance. Monarch and milkweed bug ATPases still show substantial residual activity at a millimolar ouabain concentrations.

7. A sample layout of a 96-well microtiter plate with experimental and control samples is shown in Fig. 8B.
8. Excessive dilution of Na^+/K^+-ATPase preparations before lyophilization may diminish activity or even result in a complete loss of Na^+/K^+-ATPase activity.
9. The absorbance profile has a plateau at 700–900 nm, but 700 nm is optimal (the baseline is increasing at >800 nm).
10. P_i emission and absorbance values show a linear relationship from 0 to 1.2 mM P_i in the reaction. To ensure that measured absorbance values fall within the linear range of Pi detection, a calibration curve based on KH_2PO_4 in deionized water (0.2 mM intervals, 100 μL per well for each concentration) can be used as a standard on the same plate. KH_2PO_4 standards are processed in the same way as samples.
11. Use of the *gnls()* function treats each sample dilution series as independent, giving individual noisy datapoints more weight to distort the curve fitting. Instead, curves can be fitted within a mixed-effects model framework, in which each sample dilution series is estimated as a random deviate from a universal mean curve. This approach can be implemented using the *nlme()* function in the nlme package for R. Based on prior experience, *nlme* fits are more robust with respect to technical noise, but may be more challenging to fit. Sample R code is provided in the supplementary materials. Other software, *e.g.*, Origin Pro, GraphPad Prism, or the Solver Add-in for Microsoft Excel can also be used for curve fitting.
12. This protocol can be combined with that from Section 5 to investigate inhibition of insect Na^+/K^+-ATPases by plant extracts containing cardenolides.

Acknowledgments

This work was funded by US National Science Foundation awards 1645256 to GJ and 2209762 to AA, United States Department of Agriculture – National Institute of Food and Agriculture award 2020-67013-30896 to GJ, a Triad Foundation grant to GJ, Swiss National Science Foundation grant PCEFP3_194590 to TZ, and German Research Foundation grant 2059/1-1 to GP.

References

Afolabi, M., Adegoke, G., & Mathooko, F. (2011). Phytochemical characterization of the extracts of Aframomum danielli flower, leaf, stem and root. *African Journal of Agricultural Research*, *6*, 97–101.

Agrawal, A. (2017). *Monarchs and milkweed: A migrating butterfly, a poisonous plant, and their remarkable story of coevolution*. Princeton, NJ: Princeton University Press.

Agrawal, A. A., Boroczky, K., Haribal, M., Hastings, A. P., White, R. A., Jiang, R. W., et al. (2021). Cardenolides, toxicity, and the costs of sequestration in the coevolutionary interaction between monarchs and milkweeds. *Proceedings of the National Academy of Sciences of the United States of America*, *118*.

Agrawal, A. A., Espinosa Del Alba, L., Lopez-Goldar, X., Hastings, A. P., White, R. A., Halitschke, R., et al. (2022). Functional evidence supports adaptive plant chemical defense along a geographical cline. *Proceedings of the National Academy of Sciences of the United States of America*, *119*, e2205073119.

Agrawal, A. A., Petschenka, G., Bingham, R. A., Weber, M. G., & Rasmann, S. (2012). Toxic cardenolides: Chemical ecology and coevolution of specialized plant-herbivore interactions. *The New Phytologist*, *194*, 28–45.

Agrawal, A. A., Salminen, J.-P., & Fishbein, M. (2009). Phylogenetic trends in phenolic metabolism of milkweeds (*Asclepias*): Evidence for escalation. *Evolution*, *63*, 663–673.

Alani, M. L., Younkin, G. C., Mirzaei, M., Kumar, P., & Jander, G. (2021). Acropetal and basipetal cardenolide transport in *Erysimum cheiranthoides* (wormseed wallflower). *Phytochemistry*, *192*, 112965.

Ayogu, J. I., & Odoh, A. S. (2020). Prospects and therapeutic applications of cardiac glycosides in cancer remediation. *ACS Combinatorial Science*, *22*, 543–553.

Bejcek, J., Jurasek, M., Spiwok, V., & Rimpelova, S. (2021). *Quo vadis* cardiac glycoside research? *Toxins (Basel)*, *13*.

Bock, H. (1577). *Kreutterbuch*. Straßburg: Johan Rihel.

Boff, L., Munkert, J., Ottoni, F. M., Zanchett Schneider, N. F., Ramos, G. S., Kreis, W., et al. (2019). Potential anti-herpes and cytotoxic action of novel semisynthetic digitoxigenin-derivatives. *European Journal of Medicinal Chemistry*, *167*, 546–561.

Brower, L. P., Seiber, J. N., Nelson, C. J., Lynch, S. P., & Tuskes, P. M. (1982). Plant-determined variation in the cardenolide content, thin-layer chromatography profiles, and emetic potency of monarch butterflies, *Danaus plexippus* reared on the milkweed, *Asclepias eriocarpa* in California. *Journal of Chemical Ecology*, *8*, 579–633.

Cordus, V. (1542). *Dispensatorium*. Nürnberg.

Daloze, D., & Pasteels, J. M. (1979). Production of cardiac-glycosides by Chrysomelid beetles and larvae. *Journal of Chemical Ecology*, *5*, 63–77.

Dioscorides (70AD). Περὶ ὕλης ἰατρικῆς - De Materia Medica. Anazarbus.

Dzimiri, N., Fricke, U., & Klaus, W. (1987). Influence of derivation on the lipophilicity and inhibitory actions of cardiac glycosides on myocardial Na+-K+-ATPase. *British Journal of Pharmacology*, *91*, 31–38.

Jaretzky, R., & Wilcke, M. (1932). Die herzwirksamen Glykoside von *Cheiranthus cheiri* und verwandten Arten. *Archiv der Pharmazie*, *270*, 81–94.

Klauck, D., & Luckner, M. (1995). In vitro measurement of digitalis-like compounds by inhibition of Na+/K+-ATPase: Determination of the inhibitory effect. *Pharmazie*, *50*, 395–399.

Kreis, W. (2017). The foxgloves (*Digitalis*) revisited. *Planta Medica*, *83*, 962–976.

Kreis, W., & Müller-Uri, F. (2010). Biochemistry of sterols, cardiac glycosides, brassinosteroids, phytoecdysteroids and steroid saponins. In M. Wink (Ed.), *Vol. 40. Biochemistry of plant secondary metabolism* (2nd ed., pp. 304–363). Sheffield: CRC Press.

Lopez-Goldar, X., Hastings, A., Zust, T., & Agrawal, A. (2022). Evidence for tissue-specific defence-offence interactions between milkweed and its community of specialized herbivores. *Molecular Ecology*, *31*, 3254–3265.

Luckner, M., & Wichtl, M. (2000). *Digitalis: Geschichte, Biologie, Chemie, Physiologie, Molekularbiologie, medizinische Anwendung*. Stuttgart: Wissenschaftliche Verlagsgesellschaft.

Makarevich, F. I., Zhernoklev, K. V., Slyusarskaya, T. B., & Yarmolenko, G. N. (1994). Cardenolide-containing plants of the family Cruciferae. *Chemistry of Natural Compounds*, *30*, 275–289.

Malcolm, S. (1991). Cardenolide-mediated interactions between plants and herbivores. In G. Rosenthal, & M. Berenbaum (Eds.), *The chemical participants: Vol. I. Herbivores: Their interactions with secondary plant metabolites* (2nd ed., pp. 251–296). San Diego: Academic Press.

Manna, S. K., Sreenivasan, Y., & Sarkar, A. (2006). Cardiac glycoside inhibits IL-8-induced biological responses by downregulating IL-8 receptors through altering membrane fluidity. *Journal of Cellular Physiology*, *207*, 195–207.

Mekhail, T., Kaur, H., Ganapathi, R., Budd, G. T., Elson, P., & Bukowski, R. M. (2006). Phase 1 trial of Anvirzel in patients with refractory solid tumors. *Investigational New Drugs*, *24*, 423–427.

Melero, C. P., Medarde, M., & San Feliciano, A. (2000). A short review on cardiotonic steroids and their aminoguanidine analogues. *Molecules*, *5*, 51–81.

Mijatovic, T., Mathieu, V., Gaussin, J. F., De Neve, N., Ribaucour, F., Van Quaquebeke, E., et al. (2006). Cardenolide-induced lysosomal membrane permeabilization demonstrates therapeutic benefits in experimental human non-small cell lung cancers. *Neoplasia*, *8*, 402–412.

Moon, S.-S., Rahman, A. A., Manir, M., & Ahamed, V. S. J. (2010). Kaempferol glycosides and cardenolide glycosides, cytotoxic constituents from the seeds of *Draba nemorosa* (Brassicaceae). *Archives of Pharmacal Research*, *33*, 1169–1173.

Moore, L. V., & Scudder, C. G. E. (1986). Ouabain-resistant Na, K-ATPases and cardenolide tolerance in the large milkweed bug, *Oncopeltus fasciatus*. *Journal of Insect Physiology*, *32*, 27–33.

Mori, H., Tonai-Kachi, H., Ochi, Y., Taniguchi, Y., Ohshiro, H., Takahashi, N., et al. (2009). N-(2-hydroxyethyl)-N,2-dimethyl-8-{[(4R)-5-methyl-3,4-dihydro-2H-chromen-4-yl] ami no}imidazo[1,2-a]pyridine-6-carboxamide (PF-03716556), a novel, potent, and selective acid pump antagonist for the treatment of gastroesophageal reflux disease. *The Journal of Pharmacology and Experimental Therapeutics*, *328*, 671–679.

Newman, R. A., Sastry, K. J., Arav-Boger, R., Cai, H., Matos, R., & Harrod, R. (2020). Antiviral effects of oleandrin. *Journal of Experimental Pharmacology*, *12*, 503–515.

Newman, R. A., Yang, P., Pawlus, A. D., & Block, K. I. (2008). Cardiac glycosides as novel cancer therapeutic agents. *Molecular Interventions*, *8*, 36–49.

Petschenka, G., & Agrawal, A. A. (2015). Milkweed butterfly resistance to plant toxins is linked to sequestration, not coping with a toxic diet. *Proceedings of the Biological Sciences*, *282*, 20151865.

Petschenka, G., Fandrich, S., Sander, N., Wagschal, V., Boppre, M., & Dobler, S. (2013). Stepwise evolution of resistance to toxic cardenolides via genetic substitutions in the Na+/K+-ATPase of milkweed butterflies (lepidoptera: Danaini). *Evolution*, *67*, 2753–2761.

Petschenka, G., Fei, C. S., Araya, J. J., Schroder, S., Timmermann, B. N., & Agrawal, A. A. (2018). Relative selectivity of plant cardenolides for Na(+)/K(+)-ATPases from the monarch butterfly and non-resistant insects. *Frontiers in Plant Science*, *9*, 1424.

Petschenka, G., Offe, J. K., & Dobler, S. (2012). Physiological screening for target site insensitivity and localization of Na(+)/K(+)-ATPase in cardenolide-adapted Lepidoptera. *Journal of Insect Physiology*, *58*, 607–612.

Piccioni, F., Roman, B. R., Fischbeck, K. H., & Taylor, J. P. (2004). A screen for drugs that protect against the cytotoxicity of polyglutamine-expanded androgen receptor. *Human Molecular Genetics*, *13*, 437–446.

Pierre, S. V., Yang, C., Yuan, Z., Seminerio, J., Mouas, C., Garlid, K. D., et al. (2007). Ouabain triggers preconditioning through activation of the Na+,K+-ATPase signaling cascade in rat hearts. *Cardiovascular Research*, *73*, 488–496.

Pliny the Elder (77AD). Naturalis Historia, Book 18. Rome.

Prassas, I., & Diamandis, E. P. (2008). Novel therapeutic applications of cardiac glycosides. *Nature Reviews Drug Discovery*, *7*, 926–935.

Qi, J., Zulfiker, A. H. M., Li, C., Good, D., & Wei, M. Q. (2018). The development of toad toxins as potential therapeutic agents. *Toxins (Basel)*, *10*, 336. https://doi.org/10.3390/toxins10080336.

Reddy, D., Kumavath, R., Barh, D., Azevedo, V., & Ghosh, P. (2020). Anticancer and antiviral properties of cardiac glycosides: A review to explore the mechanism of actions. *Molecules*, *25*, 3596. https://doi.org/10.3390/molecules25163596.

Shandell, M. A., Capatina, A. L., Lawrence, S. M., Brackenbury, W. J., & Lagos, D. (2022). Inhibition of the Na(+)/K(+)-ATPase by cardiac glycosides suppresses expression of the IDO1 immune checkpoint in cancer cells by reducing STAT1 activation. *The Journal of Biological Chemistry*, *101707*.

Singh, B., & Rastogi, R. P. (1970). Cardenolides—Glycosides and genins. *Phytochemistry*, *9*, 315–331.

Steyn, P. S., & van Heerden, F. R. (1998). Bufadienolides of plant and animal origin. *Natural Product Reports*, *15*, 397–413.

Tabermontanus, T. J. (1588). *Neuw Kreuterbuch*. Frankfurt: N. Bassaeus.

Taussky, H. H., & Shorr, E. (1953). A microcolorimetric method for the determination of inorganic phosphorus. *The Journal of Biological Chemistry*, *202*, 675–685.

Tverskoi, A. M., Poluektov, Y. M., Klimanova, E. A., Mitkevich, V. A., Makarov, A. A., Orlov, S. N., et al. (2021). Depth of the steroid core location determines the mode of Na, K-ATPase inhibition by cardiotonic steroids. *International Journal of Molecular Sciences*, *22*, 13268. https://doi.org/10.3390/ijms222413268.

Wang, J. K., Portbury, S., Thomas, M. B., Barney, S., Ricca, D. J., Morris, D. L., et al. (2006). Cardiac glycosides provide neuroprotection against ischemic stroke: Discovery by a brain slice-based compound screening platform. *Proceedings of the National Academy of Sciences of the United States of America*, *103*, 10461–10466.

Withering, W. (1785). *An account of foxglove and some of its medicinal uses*. London: M. Swynney.

Wong, R. W., Lingwood, C. A., Ostrowski, M. A., Cabral, T., & Cochrane, A. (2018). Cardiac glycoside/aglycones inhibit HIV-1 gene expression by a mechanism requiring MEK1/2-ERK1/2 signaling. *Scientific Reports*, *8*, 850.

Yoshida, T., Ujiie, R., Savitzky, A. H., Jono, T., Inoue, T., Yoshinaga, N., et al. (2020). Dramatic dietary shift maintains sequestered toxins in chemically defended snakes. *Proceedings of the National Academy of Sciences of the United States of America*, *117*, 5964–5969.

Zhu, Y. C. (1989). *Plantae Medicinales Chinae Boreali-Orientalis*. Harbin: Heilongjiang Science and Technology Publishing House.

Züst, T., Petschenka, G., Hastings, A. P., & Agrawal, A. A. (2019). Toxicity of milkweed leaves and latex: Chromatographic modification versus biological activity of cardenolides in 16 *Asclepias* species. *Journal of Chemical Ecology*, *45*, 50–60.

Züst, T., Strickler, S. R., Powell, A. F., Mabry, M. E., An, H., Mirzaei, M., et al. (2020). Independent evolution of ancestral and novel defenses in a genus of toxic plants (*Erysimum*, Brassicaceae). *eLife*, *9*. https://doi.org/10.7554/eLife.51712.